UNCLASSIFIED

AD 432497

DEFENSE DOCUMENTATION CENTER

FOR

SCIENTIFIC AND TECHNICAL INFORMATION

CAMERON STATION, ALEXANDRIA, VIRGINIA

UNCLASSIFIED
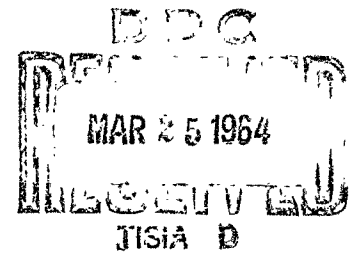
ELECTRIC-POTENTIAL TECHNIQUE

FOR DETERMINING SLOW CRACK GROWTH

by

ALBERT A. ANCTIL

ERIC B. KULA

and

EUGENE DiCESARE

MAR 2 5 1964

JTISIA D

MATERIALS TESTING LABORATORY

U. S. ARMY MATERIALS RESEARCH AGENCY

WATERTOWN, MASSACHUSETTS 02172   DECEMBER 1963

The findings in this report are not to be construed
as an official Department of the Army position.

58 0515

ELECTRIC-POTENTIAL TECHNIQUE FOR DETERMINING SLOW CRACK GROWTH

Technical Report AMRA TR 63-27

by

Albert A. Anctil

Eric B. Kula

and

Eugene DiCesare

December 1963

MATERIALS TESTING LABORATORY
U.S. ARMY MATERIALS RESEARCH AGENCY
WATERTOWN, MASSACHUSETTS 02172

U.S. ARMY MATERIALS RESEARCH AGENCY

ELECTRIC-POTENTIAL TECHNIQUE FOR DETERMINING SLOW CRACK GROWTH

ABSTRACT

Slow crack growth was followed as a function of applied load during fracture toughness testing of high-strength sheet materials by means of continuous measurement of electric potential field changes across the crack. The instrument employed is a commercially available milliohmmeter and uses the ammeter-voltmeter measurement method with a minimum of current passing through the test specimen. Voltage drop across the crack, rather than resistance, is measured. Electronic and mechanical testing techniques are described.

Typical potential field distribution diagrams illustrate the potential change with crack growth. A single calibration curve for crack size versus potential drop may be obtained independent of material and specimen configuration by maintaining geometrical similarity of current and potential contacts. Calibration data are readily obtainable for any specimen design by duplicating the specimen in aluminum foil and simulating crack growth with a razor.

Slow crack growth has been followed in 4340 and 300M steels heat treated to several strength levels as well as cold rolled and aged after heat treatment. Typical curves of load versus potential drop relate the various stages in the fracturing process.
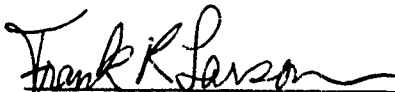
ALBERT A. ANCTIL
Mechanical Engineer

ERIC B. KULA
Physical Metallurgist

EUGENE DiCESARE
Mechanical Engineer

APPROVED:

FRANK R. LARSON
Acting Chief
Materials Testing Laboratory

CONTENTS

INTRODUCTION

In evaluating high-strength materials, it has become apparent that the standard unnotched tension test does not adequately predict the behavior of the material in actual service. The presence of sharp notches or cracks has been found to lower the performance of these materials severely. Recognizing this, the special ASTM Committee on Fracture Testing of High-Strength Metallic Materials has recommended screening tests using very sharp notches.[1] A complete analysis of the fracture of such specimens by fracture mechanics requires a knowledge not only of the load and stress intensity at which rapid crack propagation starts, but also of the size which the crack achieved by slow crack growth at the point of instability.

Several techniques have been suggested for determining one or both of the above in sheet specimens. These include visual observation and ink staining,[1] photographic,[2] sonic,[3] strain gage,[4] compliance gage,[5] and electrical resistance methods.[6] Initially, ink staining achieved greatest usage, but this technique suffers the disadvantage of being somewhat difficult to use, especially at other than room temperature. The ink tends to obscure the appearance of the fracture; but most important, the presence of the ink may itself alter the resistance to crack growth.[7] The compliance gage is currently finding greater favor.[5,8] Although capable of yielding continuous load versus crack growth data, it is relatively insensitive at small crack sizes; the modulus of elasticity must be known at the temperature of test; and the gage itself can be damaged during fracture. Steigerwald and Hanna used a Kelvin double bridge for measuring resistance.[6] This is capable of measuring very low resistances with high precision. Disadvantages are that the resistance has to be recorded manually, and heating of the specimen can occur because of the very high current used. Also, a separate calibration must be made for each material.

CRACK SIZE DETERMINATION

An electrical technique would seem to offer several advantages for studying crack sizes.[6,9-11] An electrical signal can be fed easily into an X-Y recorder and be recorded together with the load and, as in the case of the compliance gage, the complete course of the slow crack growth can be followed.

In the present investigation a commercially available milliohmmeter was used[12] which measures resistance by the ammeter-voltmeter method. The instrument uses an a-c measuring system which minimizes current through the specimen and eliminates errors due to thermal electromotive forces. The current is only 100 ma at full scale on the 0.001-ohm range. Response time is 0.25 second to 90 percent full scale, which is adequate for following slow crack growth. Contact resistance is minimized by using four terminal connections. The experimental setup is shown in Figure 1.
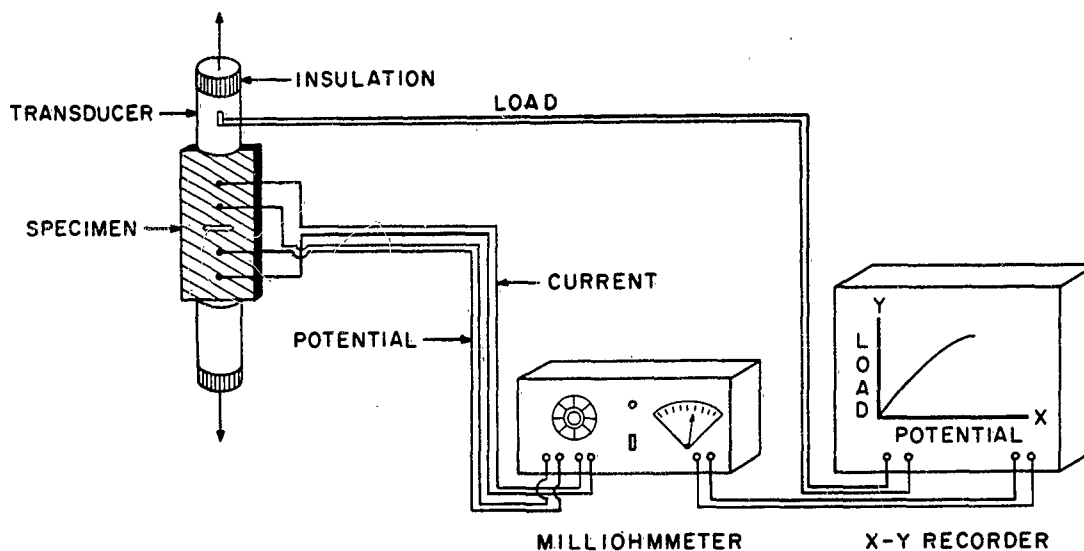
Figure I. SCHEMATIC DRAWING OF ELECTRIC-POTENTIAL MEASUREMENT AND RECORDING SETUP

Laplace's equation, $\nabla^2 \Phi = 0$, is the general equation describing the electric potential field in a specimen for any boundary conditions, specimen geometry, crack size, and location of current leads. Ohm's law then relates the potential to the resistivity and current density. Several methods for solving Laplace's equation can be found in standard texts,[13] but the direct experimental method seems best for a complicated specimen geometry. In this case a model of the test specimen was made of 0.002-inch aluminum foil. The foil was found to have a resistance high enough to be in the range of the milliohmmeter. The foil can conveniently be cut to size and the crack extended by a razor blade. Other materials including actual test specimens may be used. Experimentally determined potential fields are shown in Figure 2 for specimen configurations with and without a crack. The solid circles show the position of the current leads, and the thin black lines are the equipotential lines determined by the voltage leads.

Note that the potential changes with crack size are greatest in the region along the center line of the specimen and near the crack. The potential is also somewhat less sensitive to exact position of the leads in this region. For following the course of crack growth, the potential was measured at points marked X. It should be mentioned that the actual resistance of the specimen is not measured. The milliohmmeter supplies a constant current and the two potential leads measure a voltage drop which is converted to resistance. If all the current passed between the potential leads, the specimen resistance would be measured. However, since all the current does not flow between the potential leads, it is best to speak of potential differences rather than of resistances.

With a given geometry and constant current, the potential drop across the crack will be an accurate indication of the size of the crack. The
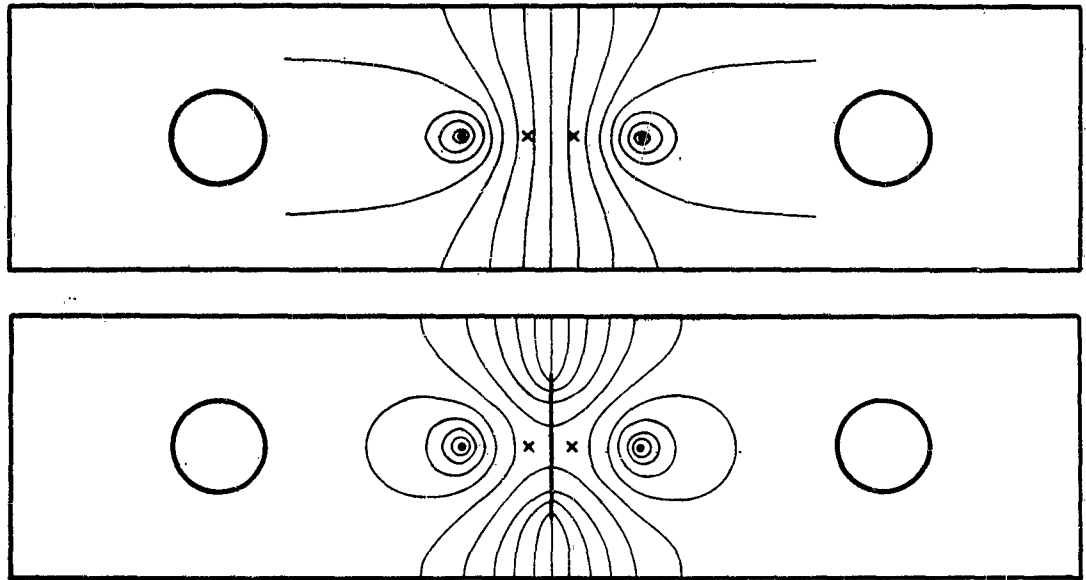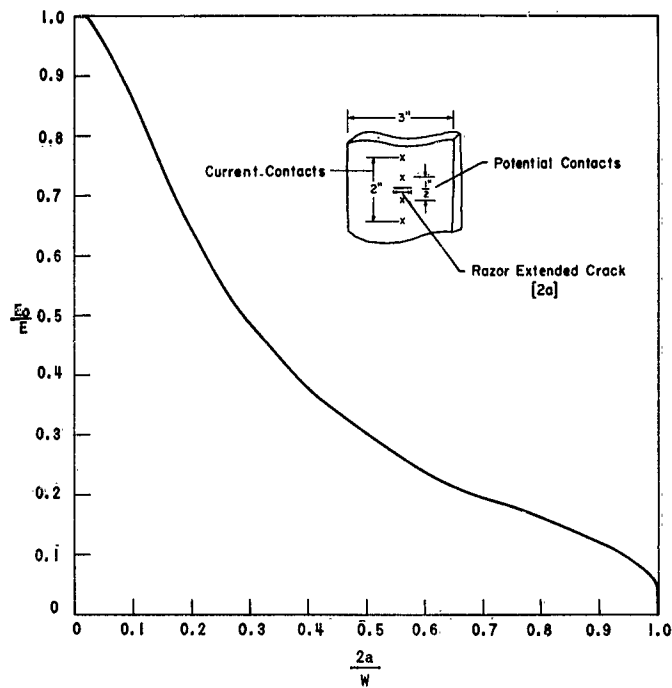
19-066-725/AMC-63

Figure 2. ELECTRIC-POTENTIAL FIELD DISTRIBUTIONS (EQUIPOTENTIAL LINES) (A)
WITHOUT A CRACK AND (B) WITH A CRACK

magnitude of the potential drop will also depend on the resistivity of the material. In order to eliminate the effects of such variables as resistivity, specimen thickness, and test temperature, a ratio of the potential drop without a crack to the potential drop with a crack, $\frac{E_O}{E}$, is taken. Figure 3 shows this ratio of voltages as a function of the crack size ratio, $\frac{2a}{W}$, for the indicated geometry. For crack sizes of interest, the measurements lie on the central portion of the curve.

The gage is made up of four Plexiglas rectangles as shown in Figure 4. The plates may contain several current and potential gage lengths to accommodate various specimen configurations. The Plexiglas could be cut out to allow observation of fatigue crack opening and subsequent slow growth during testing. Note the small vertical alignment pin, A, and lock nuts, B. Electrical contacts with the specimen are made through pointed screw heads. For elevated temperature use, some other material insulated from the specimen leads could be used for the plates.

The distance between the current leads is such that the uncracked potential drop, E_O, can conveniently be measured in the region between the machined notch and one of the pinholes before or after the test. Instead of physically moving the gage it may be more convenient, especially with tests at other than room temperature, to have an additional set of leads located at the correct distance in the region between the machined notch and the pinholes, which could be connected to the milliohmmeter immediately before and after the test.

-5-

Figure 3. CALIBRATION CURVE RELATING ELECTRIC-POTENTIAL AND CRACK SIZE
FOR CENTER-NOTCHED SPECIMENS
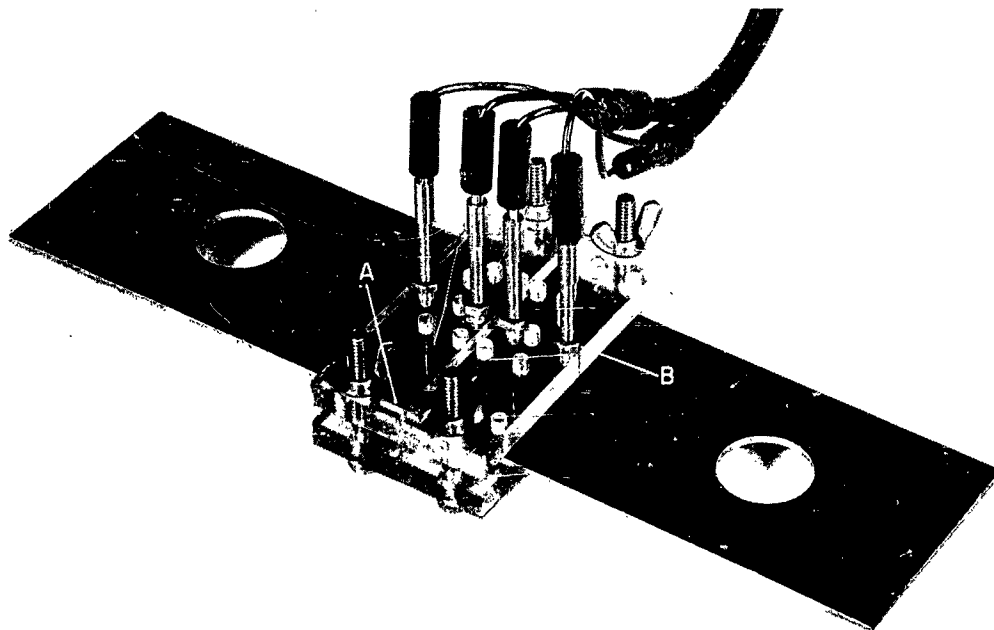
Figure 4. GAGE FOR MEASUREMENT OF ELECTRIC POTENTIAL

The calibration curve of Figure 3 was determined with an aluminum foil model of a 3-inch specimen. The same curve is valid for other specimen widths provided the distances between the crack and the current and potential leads are changed in direct proportion to the width change. This curve can also be used for edge-notched specimens since the potential fields are the same as would be obtained by taking the diagram of Figure 2B, cutting it longitudinally along the center line, and shifting the two halves so that the edges of the center notch specimen become the center line of the edge-notched specimen. In this case the potential leads can be placed at either edge, but the current leads must be divided and placed at both edges (four points).

On an actual specimen the machined notch is not razor sharp but has a finite width, since material has been removed. Because of this, the voltage drop is greater at any given crack size and the ratio $\frac{E_O}{E}$ would fall somewhat below the curve shown in Figure 3. Three calibration curves are shown in Figure 5 to illustrate this point. The upper curve was obtained
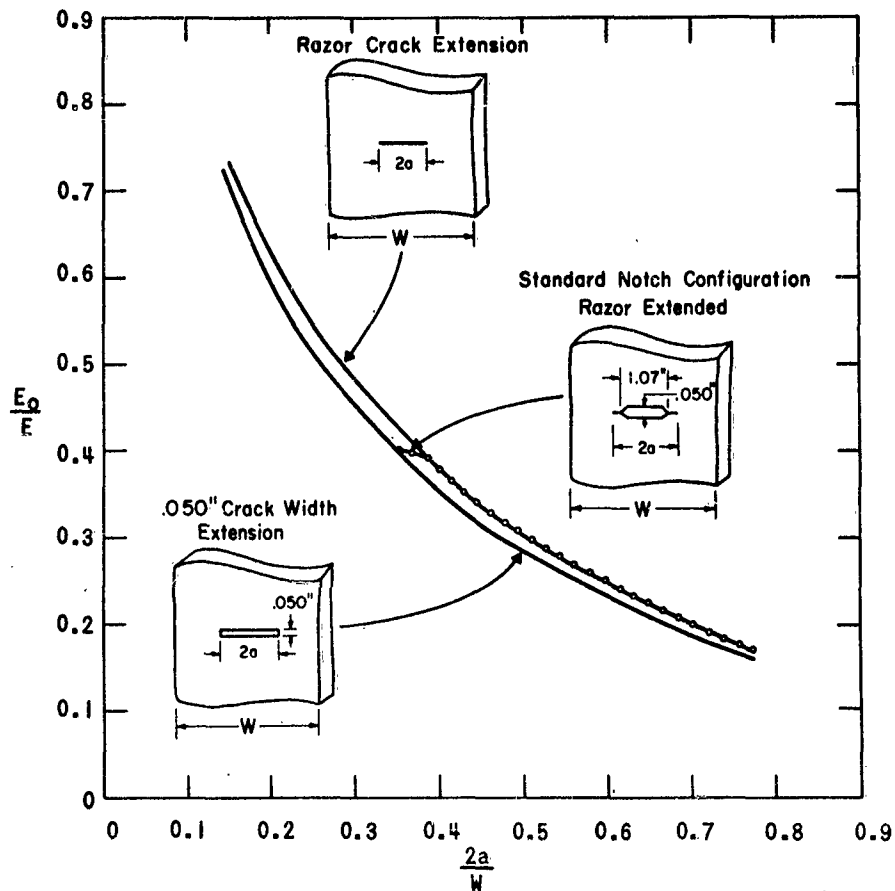

19-066-723/AMC-63

Figure 5. CALIBRATION CURVES RELATING ELECTRIC POTENTIAL AND CRACK SIZE FOR VARIOUS CRACK CONFIGURATIONS

using a razor-sharp crack. In the lower curve the notch was extended, maintaining a constant width of 0.050 inch. The transitional portion refers to the start of an actual calibration curve with an initial notch 0.050 inch wide extended by a razor cut, simulating a machined notch extended first by fatiguing and then propagating during testing. The initial ratio $\frac{E_0}{E}$ falls on or near the lower curve, then approaches the razor calibration curve rapidly and coincides with it. An extension of the 1.07-inch machined notch by only 0.110 inch is sufficient to remove the effect of the finite width of the initial machined notch.

Since the shape of the initial machined notch is not standardized, the best procedure is to determine a calibration curve starting with the particular machined notch used. The crack is then extended by a razor, and the potential drop across the crack is measured. This procedure is advisable also since a location of current and potential leads other than that shown in Figure 2 may be necessary.

The accuracy of the electric potential method was substantiated in two ways, both of which gave good agreement. The measured ratio, $\frac{E_0}{E}$, at the initiation of the elastic portion of the load-potential drop curve gave a value of crack size $\frac{2a_0}{W}$ using the calibration curve (Figure 5). This value agreed very closely with the measured fatigue crack length. A further check was made by comparing the crack length measured on heat-tinted specimens with that determined by the electric potential method for the same specimens. Agreement was within 0.015 inch; however, an accurate measurement of the heat-tinted crack length was difficult because of the lack of a sharp crack front delineation and because of its shape.

CALCULATION OF FRACTURE TOUGHNESS

In an actual test, the load is recorded as a function of the voltage drop across the crack. Typical curves, similar in shape to those shown by Steigerwald and Hanna,[6] are shown in Figure 6. First there is a reversible voltage change (specimen B7C) during elastic loading. This consists of an initial nonlinear portion, a, due to opening of the fatigue crack, followed by a linear portion, b, caused by the effect of stress on the resistivity. The curve deviates from linearity at, c, when plastic deformation or crack extension occurs and terminates at the start of fast fracture, d. In these high-strength steels changes due to plastic deformation can be neglected, and the measured deviation from the straight line portion can be attributed to crack extension. By expanding the potential drop range (millivolts) it is possible to determine crack initiation stress and type of discontinuous crack growth. Crack growth rates can be determined by plotting potential drop and load versus time.

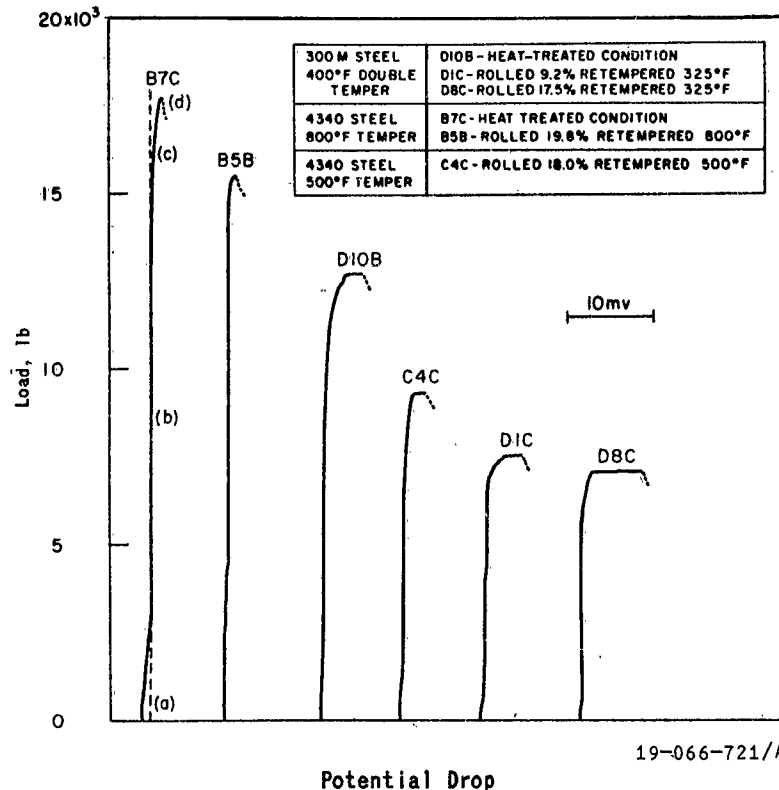The total potential change due to slow crack growth may be determined

Figure 6. TYPICAL LOAD-POTENTIAL DROP CURVES FOR 4340 AND 300M STEELS

.in a similar manner as that used to determine yield strength at a given offset percentage from an engineering stress-strain curve. The irreversible change is added to the voltage drop across the machined notch before testing plus an increment for the fatigue crack opening during testing to yield E_f, the total voltage drop across the crack in the absence of stress at the onset of rapid crack propagation. The ratio $\frac{E_o}{E_f}$ is plotted on the calibration curve (Figure 5), and the crack length, 2a, is determined from the abscissa.

This technique for measuring crack size has been used for determining the fracture toughness of 300M and 4340 steels that have been strengthened thermomechanically. Three different base strength levels are represented, 300M tempered at 400 F, and 4340 tempered at 500 and 800 F. In the tempered condition the steels were rolled various percentages at room temperature and then retempered at or slightly below the original tempering temperature. Considerable strength improvements arise from such a treatment. Heat treatments and rolling reductions are shown in Table I, together with smooth tensile and fracture toughness data. Initial thicknesses were varied and final thicknesses held constant so that all testing was carried out on sheet 0.070 inch thick. Fracture toughness specimens were 2 inches wide and fatigue cracked.

TABLE I

Tensile and Fracture Toughness Data

Specimen	Processing		Tensile Data		Fracture Data						
	Retempered (deg F)	Reduction (%)	U.T.S. (ksi)	0.2% Y.S. (ksi)	$2a_o$ (in.)	$2a$ (in.)	Shear (%)	F_{net}	F_{net} 0.2% Y.S. Ratio	K_{c_v} ksi √in.	K_{c_3} ksi √in.
4340 Steel Tempered at 800 F											
B7C	-	0	204	193	0.697	0.836	100	183	0.95	189	216
B1C	800	19.3	209	207	0.733	0.910	93	178	0.86	180	199
B5B	800	19.8	215	214	0.698	0.830	100	168	0.78	154	186
B3B	800	30.9	218	217	0.699	0.756	90	176	0.81	150	193
B3C	800	30.1	218	217	0.667	0.946	100	161	0.74	170	178
4340 Steel Tempered at 500 F											
C7C	-	0	255	221	0.693	0.934	90	179	0.81	198	204
C4C	500	18.6	279	279	0.704	0.920	100	100	0.36	88.4	104
300M Steel Tempered at 400 F											
D10B	-	0	284	229	0.682	0.868	100	142	0.62	129	152
D10C	325	0	284	229	0.684	0.900	100	145	0.63	136	151
D2C	325	6.4	310	297	0.766	0.936	88	111	0.38	94.7	113
D4B	325	7.9	320	310	0.637	0.880	76	89.3	0.28	79.4	88.7
D4C	325	7.9	320	310	0.669	0.874	92	95.0	0.31	82.3	97.0
D1C	325	9.2	316	300	0.703	0.944	75	84.5	0.28	75.1	79.8
D3B	325	9.6	321	314	0.674	0.806	79	69.0	0.22	55.6	74.8
D3C	325	8.3	321	314	0.677	0.994	79	69.4	0.22	65.2	69.0
D8C	325	17.5	338	338	0.562	1.040	71	72.8	0.22	77.3	70.7

Specimen thickness 0.070 inch, width 2.0 inches, fatigue cracked.
All specimens rolled at room temperature.
Heat treatments given. 300M - 1625 F/1 hour OQ, tempered 400 F + 400 F/1 hour.
4340 - 1700 F/1 hour AC; 1550 F/1 hour OQ.

The critical stress intensity factor, K_c, was calculated both by using the experimentally determined value of 2a to yield K_{c_v}, and by the percent shear method to obtain K_{c_3}. The net fracture stress was always less than the yield strength. The data in Table I show that K_{c_v} is a more conservative estimate of fracture toughness in almost all cases.

In measuring the flat fracture for the K_{c_3} calculations, little or no flat fracture was found for most of the specimens when measured between the recommended 1 and 2B thicknesses from the edge of the specimen; however, the amount of flat fracture was considerably greater closer to the machined notch where rapid crack propagation started. The higher values of K_{c_3} may therefore be associated with this variation in fracture appearance across the specimen width.

The results were interesting in that many of the load-voltage drop curves contained one or more portions where the crack extended under constant load as in series D and C in Figure 6. Examination during the test revealed that this crack extension occurred very rapidly compared to the extension taking place under increasing load. Several examples were noted where this accelerated growth preceded failure. Potential changes as a

function of time substantiate this measurable rate increase. This type of discontinuous crack growth was noted most frequently in the 300M steel tempered at 400 F, occasionally in 4340 steel tempered at 500 F, and not at all in the latter steel tempered at 800 F. This feature of variable crack growth appears to be associated with lower toughness levels. In some cases it was possible to relate these rapid crack extensions to steps in the fracture surface, although in many cases no correlation with the fracture surface was evident.

The effect of rolling and retempering the quenched and tempered steels was to increase the yield and tensile strengths markedly. The increase was greater the higher the initial strength level of the steel. With suf- ficiently high reduction, the yield strength equaled the tensile strength. As might be expected, the values of fracture toughness decreased as the strength level increased. Figure 7 shows the values of K_{c_V} from Table I

Symbol	Material	Rolling Temp.°F	Retempering Temp.°F
△	300M STEEL	R.T.	325
▲	400°F DOUBLE TEMPER	*	*
○	4340 STEEL	R.T.	800
●	800°F TEMPER	*	*
□	4340 STEEL	R.T.	500
■	500°F TEMPER	*	*

* Tested in Heat-Treated Condition

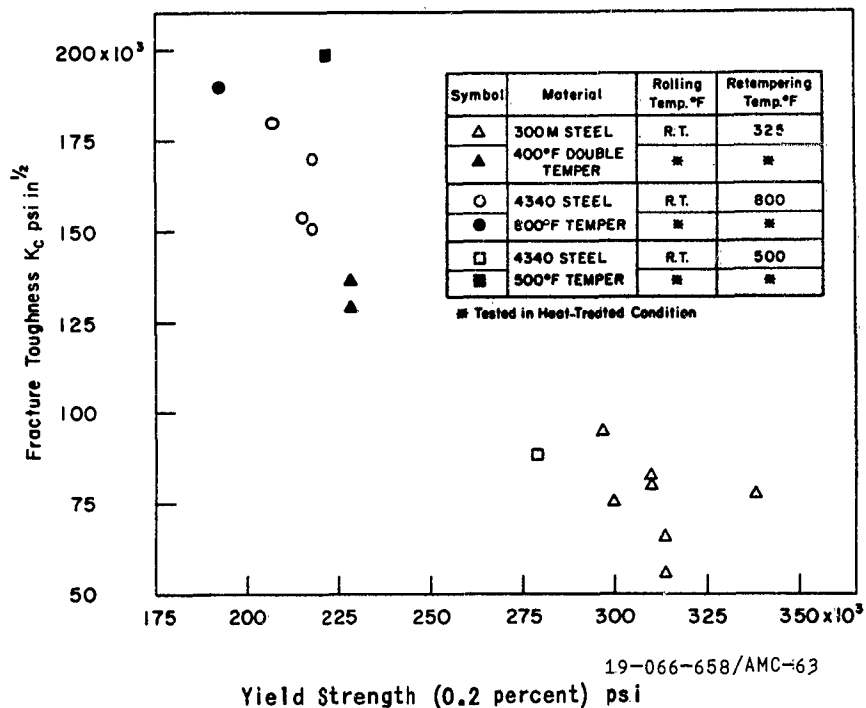19-066-658/AMC-63

Yield Strength (0.2 percent) psi

Figure 7. VARIATION OF FRACTURE TOUGHNESS WITH YIELD STRENGTH FOR 4340 AND 300M STEELS

plotted against the yield strengths. There is a general scatter band show- ing the decrease in toughness with increase in strength level. Although it had been hoped that certain thermomechanical treatments would show better strength-toughness combinations than others, the scatter in the data precludes such conclusions.

SUMMARY

Slow crack growth in sheet tension specimens can be followed by measurement of the electric potential across the crack. The signal from a commercially available milliohmmeter is fed into a recorder to obtain load-potential drop or potential drop-time curves. Calibration of the potential drop with crack size can be made with measurements on aluminum foil cut to the shape of the specimen and with the crack extended by cutting with a razor. The calibration procedure is applicable to any type of potential measurement circuit. This method of determining crack size offers advantages over other methods in that it is relatively easy to make the measurements, the slow crack growth can be continuously followed, and a calibration of the potential drop with crack size can readily be made.

Using this technique, fracture toughness was determined in 300M and 4340 steels which, in the quenched and tempered condition, had been cold rolled and aged. Although significant strength increases were obtained by this treatment, the fracture toughness was severely lowered.

REFERENCES

1. Fracture Testing of High Strength Sheet Materials. Report of Special ASTM Committee, ASTM Bulletin No. 243, January, 1960, p. 29-40, and No. 244, February 1960, p. 18-28.

2. GERBERICH, W. W. Fracture Toughness of SAE 4340 Steel Heat-Treated to 200,000 to 300,000 psi Yield Strengths. Jet Propulsion Laboratory, Technical Report No. 32-96, Pasadena, California, April 1961.

3. ROMINE, H. E. Determination of the Driving Force for Crack Initiation from Acoustic Records of G_c Tests on High-Strength Metals for Rocket Motor Casings. NWL Report No. 1779, 4 October 1961.

4. BOYLE, R. W., SULLIVAN, A. M., and KRAFFT, J. M. Determination of Plane Strain Fracture Toughness with Sharply Notched Sheets. ASME Preprint 62-Met-13.

5. KRAFFT, J. M., and SULLIVAN, A. M. Notes on Status of Fracture Mechanics Research at NRL, ASTM-FTHSSM Committee Meeting at Washington, February 1962.

6. STEIGERWALD, E. A., and HANNA, G. L. Initiation of Slow Crack Propagation in High-Strength Materials. Proceedings, ASTM, v. 62, 1962, p. 885.

7. STEIGERWALD, E. A. Delayed Failure of High-Strength Steel in Liquid Environments. Proceedings, ASTM, v. 60, 1960, p. 750.

8. BOYLE, R. W. A Method for Determining Crack Growth in Notched Sheet Specimens. Materials Research and Standards, v. 2, no. 8. August, 1962, p. 646.

9. BARNETT, W. J., and TROIANO, A. R. Crack Propagation in the Hydrogen Induced Brittle Fracture of Steel. Journal of Metals, v. 9, April, 1957, p. 486; Transactions, AIME, v. 209, April, 1957, p. 486-494.

10. SCHMIDT, R. E. Electrical Resistance as an Indication of Fuel Element Crack. Atomic Energy Commission Report No. DC-60-11-103, November, 1960.

11. LYST, J. O., and BABILON, C. F. Detecting Fatigue Cracks in Notched Fatigue Specimens by Changes in Electrical Resistance. Materials Research and Standards, v. 2, no. 6, June, 1962, p. 485.

12. Keithley Instruments Inc., Keithley Engineering Notes, v. 10, no. 1, January, 1962.

13. MOON, P., and SPENCER, D. E. Field Theory for Engineers. D. Van Nostrand Co., Inc., New York, 1961.

AD

Accession No.

U.S. Army Materials Research Agency, Watertown, Massachusetts 02172 — ELECTRIC-POTENTIAL TECHNIQUES FOR DETERMINING SLOW CRACK GROWTH — Albert A. Anctil, Eric B. Kula and Eugene DiCesare

Technical Report AMRA TR 63-27, December 1963, 13 pp - table, illus, AMCMS Code 5025.11.84202, D/A Project 1A024401A11002, Unclassified Report

Slow crack growth was followed as a function of applied load during fracture toughness testing of high-strength sheet materials (4340 and 300M steels) by means of continuous measurement of electric potential field changes across the crack. Electronic and mechanical testing techniques are described. Typical potential field distribution diagrams illustrate the potential change with crack growth. A single calibration curve for crack size versus potential drop may be obtained independent of material and specimen configuration by maintaining geometrical similarity of current and potential contacts. Calibration data are readily obtainable for any specimen design by duplicating the specimen in aluminum foil and simulating crack growth with a razor. NO DISTRIBUTION LIMITATIONS

NO DISTRIBUTION LIMITATIONS